Heliyon 10 (2024) e27145

Contents lists available at ScienceDirect

Heliyon

journal homepage: www.cell.com/heliyon

Research article

# Phytochemical composition of Tibetan tea fermented by Eurotium cristatum and its effects on type 1 diabetes mice and gut microbiota

Junlin Deng [a,1], Kebin Luo [a,b,1], Chen Xia [a,1], Yongqing Zhu [a], Zhuoya Xiang [a], Boyu Zhu [a], Xiaobo Tang [c], Ting Zhang [c], Liugang Shi [d], Xiaohua Lyu [b,**], Jian Chen [a,*]

[a] Institute of Agro-Products Processing Science and Technology, Institute of Food Nutrition and Health, Sichuan Academy of Agricultural Sciences, Chengdu, 610066, China
[b] Department of Nutrition and Food Hygiene, West China School of Public Health and West China Fourth Hospital, Sichuan University, Chengdu, 610041, China
[c] Tea Research Institute, Sichuan Academy of Agricultural Sciences, Chengdu, 610066, China
[d] Yazhou Hengtai Tea Industry Co. LTD, Sichuan, Ya'an, 625100, China

ARTICLE INFO

*Keywords:*
Theabrownin
Tibetan tea extract
Eurotium cristatum fermentation
Diabetes mellitus
Gut microbiota

ABSTRACT

"Golden-flower" Tibetan tea (GTT) is an innovative dark tea fermented via fungus Eurotium cristatum. To study GTT effects on alleviating the symptoms of type 1 diabetes mellitus (T1DM), GTT's extract (GTTE) was prepared. GTTE chemical compositions were analyzed via HPLC, pyrolysis-gas chromatography-mass (Py-GC-MS) spectrometry analysis, and chemistry analyses. GTTE effects on T1DM were explored on T1DM mice model induced by streptozotocin (STZ). GTTE was composed mainly of tea pigment theabrownin (TB) (49.18%), with high percentages of polysaccharide (16.93%), protein (10.15%), polyphenols (13.90%), amino acids (5.89%), caffeine (1.83%), and flavonoids (0.67%). Py-GC-MS results exhibited that GTTE constituted of phenols, lipids, sugars, and proteins. GTTE attenuated T1DM conditions of mice, relieved their liver and pancreatic injury, restored damaged islet cells, decreased oxidative stress by increasing superoxide dismutase (SOD) and catalase (CAT) levels, modulated cytokine expression leading to the decreasing pro-inflammatory cytokines TNF-α and IL-6, increased anti-inflammatory cytokines IL-4 to improve inflammatory responses, and optimized gut microbiota composition and structure based on high-throughput 16S rDNA sequencing, suggesting multi-channel anti-diabetes mechanisms.

## 1. Introduction

Diabetes mellitus (DM) is a complex metabolic disorder characterized by hyperglycemia caused by the defects in insulin secretion, insulin action, or both. Long-time complications caused by DM increase the hazards of this disease as well, such as the long-term

* Corresponding author.
** Corresponding author.
*E-mail addresses:* luxiaohua@scu.edu.cn (X. Lyu), jc_saas@yahoo.com (J. Chen).
[1] Contribute equally.

https://doi.org/10.1016/j.heliyon.2024.e27145
Received 2 June 2023; Received in revised form 14 February 2024; Accepted 25 February 2024
Available online 27 February 2024

damage, dysfunction, and failure of different organs, especially the eyes, kidneys, nerves, heart, and blood vessels [1]. There are two types of diabetes mellitus, Type 1 and Type 2. Type 1 diabetes mellitus (T1DM) is caused by the absolute insulin deficiency associated with autoimmune-mediated destruction of pancreatic β-cells islets. T1DM patients regularly take exogenous insulin to prevent the development of ketoacidosis for survival [2]. Although T1DM composes of about ten percent of the diabetic population, it is more difficult for people to overcome or alleviate T1DM than Type 2 diabetes mellitus (T2DM). There are many challenges for the prevention and treatment to T1DM as according to the recent report in *The Lancet* [3].

In addition to the variety of medicines being used for the treatment of diabetes, herbs and botanicals, such as dietary supplements, are also used for glycemic control and management of diabetic complications [4]. Most plants generate bio-active natural substances including polyphenols, flavonoids, terpenoids, coumarins, and glycosides, some of which were reported to have anti-diabetic effects [5].

Tea (Camellia sinensis L.), derived from the leaves or buds of tea trees, has a long history of more than 5000 years in dietary and medicinal applications [6]. Nowadays, tea has become more and more popular due to its attractive aroma, taste and health-promoting benefits, such as antioxidant, anticancer, anti-inflammatory, immunomodulatory, and hypoglycemic activities [7–10]. According to the post-harvest processing and the degree of fermentation, tea products are generally classified into five major categories in China, i.e., unfermented (green tea), slight-fermented (white tea and yellow tea), semi-fermented (Oolong tea), fermented (black tea), and the post-fermented (dark tea) [11]. The difference lies in the degree of fermentation, which results from oxidative, enzymatic changes, or microbial fermentation within the tea leaves during the manufacturing process [12]. There are significant differences in the active components in the various types of teas. Catechins are the predominant polyphenolic compounds in green tea. Tea pigments theaflavin and thearubigin are present in high concentrations in black tea whereas, theabrownin (TB), is the main tea pigment with various bio-activities in dark tea [13,14].

Tibetan tea is a dark tea in China originally made in Ya'an city area of Sichuan Province. This tea has existed for thousands of years and is deeply loved by the Tibetans. Tibetans live in the Qinghai-Tibet Plateau, an area with extreme cold, hypoxia, and intense UV radiation. The Tibetan eating habits consist of long time high-fat foods and less dietary fiber. Because Tibetan tea is rich in polyphenols, polysaccharides, trace elements, free amino acids and other components [15]. Tibetan tea is helpful for Tibetan digestion and health, as the saying "the energy of meat can't be digested without Tibetan tea, the heat of hulless barley can't be dispelled without Tibetan tea" [16]. In recent decades, the application of an innovative post-fermentation process has caused dominate fungi probiotic Eurotium cristatum yellow flora to grow on both brick and loose forms of Tibetan tea, causing the tea to possess many specific "golden flowers" in the dark tea. Nowadays, drinking the "golden flower" Tibetan tea (GTT) has become popular among Chinese people. However, there are few research reports of its antidiabetic effect, especially on its effects on the treatment of T1DM. The aims of this paper are to study and elucidate the phytochemical compositions of the extract of the "golden flower" Tibetan tea (GTTE), and to investigate its effects on T1DM mice model and the influence on gut microbiota profiles. This research provides deep insights of the phytochemical components of drinking from GTT, potential supplementary health benefits on T1DM, and the possible mechanisms.

## 2. Materials and methods

The "golden-flower" Tibetan tea (GTT) bricks (batch no. 20100619) were made from tea leaves and hubs (Camellia sinensis L.) that were post-fermented for 10 years with the growing Eurotium cristatum yellow flora (from Ya'an Golden Flower Tibetan Tea Corporation).

### *2.1. Reagents and standards*

Metformin (DMBG) was purchased from Sino-American Shanghai Squibb Pharmaceuticals Co., Ltd. The superoxide dismutase (SOD) kit and catalase (CAT) kit were obtained from Nanjing Jiancheng Biotechnology Co., Ltd. Multi-factor detection kit was purchased from American R&D company. Insulin ELISA kit was purchased from American Millipore Co., Ltd. Paraformaldehyde (4%) was purchased from Beijing Soleibo Technology Co., Ltd. Streptozotocin (STZ) was obtained from American Sigma Company. Gallic acid (GA), Catechin (C), Epicatechin (EC), Gallocatechin (GC), Epigallocatechin (EGC), Catechin gallate (CG), Epicatechin gallate (ECG), Gallocatechin gallate (GCG), Epigallocatechin gallate (EGCG), purity of up to 98%, were purchased from Beijing Solarbio Science & Technology Co., Ltd.

Instruments and apparatuses were used in the studies included the following: CR21 N high-speed refrigerated centrifuge (Hitachi Co., Ltd., Japan), RM2235 paraffin microtome (Leica Co., Ltd., Germany), Eclipse Ci- L upright fluorescence photo microscope (Nikon Co., Ltd., Japan), MV752 N UV–Vis spectrophotometer (Shanghai Youke instrument Co., Ltd. China), Analysis platform (Millipore Co., Ltd., USA), Eclipse Ci-L upright white light photo microscope (Nikon Co., Ltd., Japan), Eclipse Ci-L upright polarized light photo microscope (Nikon Co., Ltd., Japan), Eclipse Ti-E laser confocal microscope (Nikon Co., Ltd., Japan), PANNORAMIC DESK/MIDI/250/1000 panoramic slide scanner (3DHISTECH Ltd., Hungary); 2.5\10\20\200\1000\5000 μL pipette (Eppendorf Ltd., Germany).

### 2.2. Preparation of "golden-flower" Tibetan tea extract (GTTE)

The dry powder of "golden-flower" Tibetan tea (5875 g) was homogenized with 58.75 L water and extracted at 75 °C for 2 h. The supernatant was decanted and retained. The residue was further extracted twice at 75 °C for 1 h and 0.5 h, respectively. Then, the three extracted supernatants were combined and evaporated under vacuum at 50 °C on a rotary evaporator (Hei-VAP; Heidoiph Instruments, Schwabach, Germany), until the volume was reduced to 1/5 of the original volume. The remaining aqueous phase was mixed with anhydrous ethanol (1/4, v/v), and then precipitated at 4 °C for 24 h. The precipitate was collected and dissolved in distilled water. The solution was finally frozen-dried to obtain 682.5 g of brown extract powder with the yield of 11.62%. This water-extraction alcohol-precipitation extract of "golden-flower" Tibetan tea (GTTE) was used for the following experiments.

### 2.3. Phytochemical composition analyses of GTTE

#### 2.3.1. Determination of polysaccharides, total phenols, total flavonoids, amino acids, protein and tea pigments

The polysaccharide content was determined by the phenol-sulfuric acid method using dextrose as a standard [17]. The protein content was measured by Coomassie Brilliant Blue method using bovine serum albumin as reference. The amino acids were determined according to a national standard GB5009.124–2016 method of China. The total polyphenols content was determined by the Folin-Ciocalteu method using gallic acid as a standard [18]. The total flavonoids content was determined by the AlCl3 colorimetric method with rutin as a standard [19]. The contents tea pigments, i.e., theaflavin, thearubigin, and theabrownin (TB) were determined using Roberts colorimetric method [17].

The analyses of nine phenolic compounds (GA, C, EC, GC, EGC, CG, ECG, GCG and EGCG) and caffeine were performed using an Agilent LC-1290 UHPLC system (Agilent, USA, Santa Clara, CA, USA) equipped with a diode array detector (DAD). Chromatographic separation was conducted on a Waters BEH C18 (2.1 × 100 mm, 1.7 μm; Waters Corporation; Milford, MA, USA). The mobile phase consisted of water soluble with 1% formic acid (A) + acetonitrile (B). The gradient program was set at 0–2 min (5%–10% B), 2–10 min (10%–20% B), 10–15 min (20%–40% B), 15–17 min (40%–70% B), 17–20 min (70% B–95% B) using a flow rate of 0.3 mL/min. The column temperature was 30 °C; the detection wavelength was 280 nm. Samples were filtered using a 0.22 μm membrane filter and the injection volume was 1 μL. The calibration for the quantification of the nine phenolic compounds and caffeine is exhibited in Supplementary Material S1 Table 1.

#### 2.3.2. Pyrolysis-gas chromatography-mass (Py-GC-MS) spectrometry analysis of GTTE

The Pyrolysis-gas chromatography-mass (Py-GC-MS) (Shimadzu PY2020, Japan) was used to determine the thermal decomposition fragments of GTTE, especially that of tea pigment TB. The Py-GC-MS conditions were programed as following: pyrolysis time 10 s, at the pyrolysis chamber temperature 380 °C and 600 °C, respectively, injection needle temperature 380 °C. J&W DB-5 quartz capillary column (30 m) was used to separate the compounds. The analysis was conducted via programmed temperature: 60 °C (5 min), 60–280 °C at 10 °C/min (8 min), 280–380 °C at 5 °C/min (2 min). Carrier was helium gas, and flow rate was 5.0 mL/min. MS conditions: ion source temperature 220 °C, transmission line temperature 270 °C, electron ionization source and electron energy 70 eV, scanning time 0.2 s, quality scan range 50–500. The area normalization method was used to determine the relative content of decomposing substances.

**Table 1**
The phytochemical component of GTTE.

| Conventional composition ( g/100g ) | | Tea pigment ( g/100g ) | | Phenolic compound ( g/100g ) | | Amino acid ( g/100g ) | |
|---|---|---|---|---|---|---|---|
| Tea polysaccharide | 16.93 ± 0.2 | Theabrownin | 49.18 ± 0.28 | GA | 0.48 ± 0.00 | Aspartate | 0.75 ± 0.01 |
| Protein | 10.15 ± 0.11 | Theaflavin | 0.25 ± 0.03 | EGC | 0.06 ± 0.00 | Threonine | 0.36 ± 0.01 |
| Total amino acids | 5.89 ± 0.01 | Thearubigin | ND | C | 0.05 ± 0.00 | Serine | 0.46 ± 0.00 |
| Total polyphenols | 13.90 ± 0.65 | – | – | EGCG | 0.03 ± 0.00 | Glutamate | 1.04 ± 0.02 |
| Total flavonoids | 0.67 ± 0.00 | – | – | GCG | 0.01 ± 0.00 | Glycine | 0.44 ± 0.01 |
| Caffeine | 1.83 ± 0.00 | – | – | EC | 0.11 ± 0.00 | Alanine | 0.23 ± 0.01 |
| | | – | – | ECG | 0.06 ± 0.00 | Valine | 0.28 ± 0.01 |
| – | – | – | – | CG | 0.01 ± 0.00 | Methionine | 0.16 ± 0.00 |
| – | – | – | – | GC | 0.51 ± 0.00 | Isoleucine | 0.15 ± 0.00 |
| – | – | – | – | – | – | Leucine | 0.27 ± 0.01 |
| – | – | – | – | – | – | Tyrosine | 0.19 ± 0.00 |
| – | – | – | – | – | – | Phenylalanine | 0.17 ± 0.01 |
| – | – | – | – | – | – | Lysine | 0.32 ± 0.01 |
| – | – | – | – | – | – | Histidine | 0.29 ± 0.01 |
| – | – | – | – | – | – | Arginine | 0.14 ± 0.01 |
| – | – | – | – | – | – | Proline | 0.34 ± 0.02 |

ND, not detected.

### 2.4. Animals and experiments

#### 2.4.1. Animal experiments

The GTTE was used as test sample. A total of 70 male mice from Institute of Cancer Research (ICR), weighing 20–24 g (7–8 weeks old), were purchased from Beijing Vital River Laboratory Animal Technology Co., Ltd. (Certificate Number SCXK [zhe] 2019-0001; Beijing, China). They were adaptive having free access to feed (normal feed nutrition see Supplementary Material S2 Table 2) and water (one mouse per cage) in an environmentally controlled room (temperature 22 ± 1 °C, relative humidity 55%–60%, 12 light/dark cycle) for two weeks. The study was approved by Animal Care and Use Committee (Approval No. KS20201023), Sichuan University, China.

The type 1 diabetes in mice was induced via intraperitoneal administration of Streptozotocin (STZ) (130 mg/kg BW) in citric acid/sodium citrate buffer (0.1 mol/L, pH 4.2–4.5) [20]. Simultaneously, the normal mice were administered equivalent citrate buffer. The normal control (NC) group and the high-dose normal group were given equal doses of citrate buffer. After STZ administration for 7 days, fasting blood glucose (FBG) was detected via a tail vein nick. The mice were considered as successful diabetic models when their FBG was greater than 8.3 mmol/L [21], and with typical diabetes symptoms of polyuria, polydipsia, polyphagia, and weight loss. The diabetic model mice were divided randomly into five groups: diabetic control group (DC, n = 7), positive control group (PC, 333 mg/kg BW Metformin, n = 7), and three dosage groups, i.e., diabetic mice with high dose GTTE group (TH, 900 mg/kg BW GTTE, n = 7), diabetic mice with medium dose GTTE group (TM, 450 mg/kg BW GTTE, n = 7), and diabetic mice with low dose GTTE group (TL, 225 mg/kg BW GTTE, n = 7). The dosages were designed according to a reference of tea pigment capsule study [22]. Meanwhile, normal mice were randomly divided into two groups: normal control group (NC, n = 7), nondiabetic with GTTE group (NDT, 900 mg/kg BW GTTE, n = 7). During the experimental period, fasting blood glucose, body weights and feed intake were measured weekly. Their body weights were weighed weekly to adjust gavage dose, and their behaviors were observed. At the end of the 28 days of experimental period, feces were collected on the day before their sacrifice and stored at −80 °C. Mice were fasted for 12 h and then sacrificed. Blood samples were collected and centrifuged at 3500 rpm for 15 min to gain serum for subsequent analyses. In addition, kidneys, livers, and pancreas of the mice were immediately taken and stored at −80 °C.

**Table 2**
Pyrolysis-gas chromatography-mass spectrometry (Py-GC-MS) analysis of GTTE at 380 °C.

| No. | Rt (min)[a] | Compound | CAS No. | Content (%) [b] | SI [c] |
|---|---|---|---|---|---|
| 1 | 1.342 | Ethylamine | 75-12-7 | 16.73 | 94 |
| 2 | 1.415 | 5-Amino-6-nitroso-2,4(1H,3H)-pyrimidin | 0-00-0 | 7.02 | 95 |
| 3 | 1.466 | Ethanol | 64-17-5 | 10.45 | 97 |
| 4 | 1.565 | 3-oxo-Butanenitrile | 0-00-0 | 9.97 | 92 |
| 5 | 1.879 | 2,3-Butanedione | 431-03-8 | 2.04 | 98 |
| 6 | 2.048 | Acetic acid | 64-19-7 | 11.82 | 97 |
| 7 | 2.340 | Furan | 1708-29-8 | 0.45 | 79 |
| 8 | 2.390 | 1-hydroxy-2-Propanone | 116-09-6 | 4.77 | 98 |
| 9 | 2.717 | 2,3-Pentanedione | 600-14-6 | 0.48 | 95 |
| 10 | 2.810 | Propanoic acid | 79-09-4 | 0.26 | 83 |
| 11 | 2.878 | 3-hydroxy-2-Butanone | 513-86-0 | 0.43 | 95 |
| 12 | 2.920 | 2,4-Dimethylfuran | 3710-43-8 | 0.43 | 89 |
| 13 | 5.622 | 2-Furanmethanol | 98-00-0 | 0.91 | 96 |
| 14 | 5.904 | 1-(acetyloxy)-2-Propanone | 592-20-1 | 0.60 | 97 |
| 15 | 9.273 | Phenol | 108-95-2 | 0.58 | 95 |
| 16 | 10.055 | 5-Methyl-5,6-dihydro-2(1H)-pyridinone | 0-00-0 | 0.16 | 86 |
| 17 | 11.544 | Cyclopropyl carbinol | 2516-33-8 | 0.32 | 88 |
| 18 | 12.778 | Xanthine riboside | 146-80-5 | 0.36 | 89 |
| 19 | 14.444 | Methyl pentadecyl ether | 0-00-0 | 0.40 | 72 |
| 20 | 14.552 | 2-[(tetrahydro-2H-pyran-2-yl)oxy]- Propanoic acid | 87930-86-7 | 0.50 | 78 |
| 21 | 14.850 | 2,5-Monomethylene-*l*-rhamnitol | 0-00-0 | 0.31 | 68 |
| 22 | 17.425 | 1,1′-oxybis-Octane | 629-82-3 | 0.33 | 92 |
| 23 | 17.563 | 1-Tetradecanol | 112-72-1 | 0.37 | 86 |
| 24 | 18.291 | Octanoic acid, octyl ester | 2306-88-9 | 0.11 | 92 |
| 25 | 19.013 | Caffeine | 58-08-2 | 29.47 | 95 |
| 26 | 19.595 | Dibutyl phthalate | 84-74-2 | 0.39 | 95 |
| 27 | 20.412 | 1-Hexadecanol | 36653-82-4 | 0.11 | 92 |
| 28 | 20.935 | Propionic acid, 3,3′-thiodi-, didodecyl | 123-28-4 | 0.03 | 68 |
| 29 | 21.256 | Octanoic acid, 4-pentadecyl ester | 0-00-0 | 0.03 | 76 |
| 30 | 22.192 | Hexanedioic acid, bis(2-ethylhexyl) ester | 103-23-1 | 0.04 | 90 |
| 31 | 22.813 | Oxalic acid, 2-ethylhexyl isohexyl ester | 0-00-0 | 0.04 | 83 |
| 32 | 23.050 | Diisooctyl phthalate | 131-20-4 | 0.05 | 92 |
| 33 | 23.418 | Heptyl tetracosyl ether | 0-00-0 | 0.04 | 78 |

Note.
[a] Rt, retention time of pyrolytic product.
[b] The relative contents of pyrolytic products were calculated by peak area normalization, and results are expressed as the ratio of single constituent area to total area.
[c] SI, index of similarity.

*2.4.2. Measurement of body weight, fasting blood glucose (FBG), and oral glucose tolerance test (OGTT)*

Body weight of each group was measured once a week (0 W, 1 W, 2 W, 3 W, 4 W, and 5 W) in 5 weeks. The fasting blood glucose (FBG) was determined using Accu-Chek Performa (Roche Diagnostics, Mannheim, Germany) blood glucose meter from the tail vein after overnight fasting at 1 W and 5 W.

The oral glucose tolerance test (OGTT) was carried on the day of mice euthanized. The mice were fasted for 4 h (without water) after the last intragastric administration. The 10 mL of glucose (Sigma-Aldrich Co.) solution (2 g/kg) was performed by gastric perfusion. Subsequently, the blood sample were taken from their tail vine, and blood glucose level was determined using Roche blood glucose meter at 30, 60, 90, and 120 min.

*2.4.3. Serum insulin test*

The blood samples were centrifuged for 15 min at 3500 rpm to obtain the serum for following assays. The content of insulin in serum was detected according to the enzyme-linked immunosorbent assay in the ELASA kit (Millipore Inc., USA).

*2.4.4. Organ index of kidney, liver, and pancreas*

Weights of kidney, liver, and pancreas were measured to calculate the indexes of these organs, as the ratio of organ mass (g) to body mass (g).

*2.4.5. Liver and serum antioxidant assay*

Liver tissues were homogenized with physiological saline (1/9, w/v), then centrifuged by 3000 rpm for 10 min at 4 °C. The supernatants were used to determine the liver biochemical indicators, i.e., superoxide dismutase (SOD) and catalase (CAT) levels, for assays of antioxidant, using commercial kits (Nanjing Jiancheng Bioengineering Institute, China). Serum antioxidant assays were also using the kits.

*2.4.6. Histopathological observation of liver and pancreas*

Hepatic tissue and pancreatic tissue were fixed with paraformaldehyde, dehydrated by gradient ethanol, wrapped in wax, sectioned into 5 μm sections, dewaxed in xylene, and hydrated by gradient ethanol. All specimens were stained through hematoxylin-eosin staining, and sealed with neutral resin to observe histomorphological changes using optical microscopy.

*2.4.7. Determination of serum inflammatory factors*

Three serum samples were randomly selected from each group. The levels of pro-inflammatory cytokines TNF-α, IL-6, and anti-inflammatory cytokines IL-4 in the serum samples were detected using multi-factor detection kits (US R&D Company).

*2.4.8. Determination of islet β-cell area*

Three pancreatic tissues were randomly selected from each group, which were embedded with wax and sliced for immunofluorescence double staining. The sections were incubated with specific primary antibodies against insulin and glucagon. Subsequently, sections were incubated with FITC-labeled goat anti-Rabbit IgG + IgM and TRIT-Labeled Goat anti-mouse IgG + IgM, and then observed with a fluorescence microscope (Eclipse Ci-L, NIkon LTD., Japan).

*2.4.9. High-throughput 16S rDNA sequencing of gut microbiota*

The feces of mice were collected on the day before sacrifice and stored at −80 °C for 16S rDNA sequencing. Total genomic DNA from samples was extracted via CTAB/SDS method. DNA concentration and purity were monitored on 2% agarose gels. Then, the V3–V4 variable regions of the bacterial 16S rDNA gene were amplified with universal primers (ACTCCTACGGGAGGCAGCA and GGACTACHVGGGTYGTTECTAAT). The PCR products were recovered for fluorescence quantification using AxyprepDNA Gel Extraction Kit (AXYGEN). Sequencing libraries were generated using NEB Next®Ultra™DNA Library Prep Kit for Illumina (NEB, USA) following manufacturer's recommendations and index codes were added. The library quality was assessed on the Qubit@ 2.0 Fluorometer (Thermo Scientific) and Agilent Bioanalyzer 2100 system. At last, the library was sequenced on an Illumina NovaSeq 6000 platform and 250bp paired-end reads were generated by Shanghai Applied Protein Technology Corp. (Shanghai, China).

The 16S sequences analysis was performed by UPARSE software package using the UPARSE-OTU and UPARSE-OTUref algorithms. In-house Perl scripts were used to analyze alpha (within samples) and beta (among samples) diversity. Sequences with ≥97% similarity were assigned to the same OTUs. We pick a representative sequences for each OTU and use the RDP classifier to annotate taxonomic information for each representative sequence. In order to compute Alpha Diversity, we rarify the OTU table and calculate three metrics: Chao1 estimates the species abundance; Observed Species estimates the amount of unique OTUs found in each sample, and Shannon index.

Graphical representation of the relative abundance of bacterial diversity from phylum to species can be visualized using Krona chart. Cluster analysis was preceded by principal component analysis (PCA), which was applied to reduce the dimension of the original variables using the QIIME software package. QIIME calculates both weighted and unweighted unifrac distance, which are phylogenetic measures of beta diversity. We used unweighted unifrac distance for Unweighted Pair Group Method with Arithmetic mean (UPGMA) Clustering，which is a type of hierarchical clustering method using average linkage and can be used to interpret the distance matrix.

To identify differences of microbial communities between the two groups, ANOSIM and ADONIS were performed based on the Bray-Curtis dissimilarity distance matrices. Based on the relative abundance of identified differential abundant bacterial group, gut microbiota composition were analyzed at phylum level and genus level.

### 2.5. Statistical analysis

All results were expressed as mean ± standard deviation (SD). One-way analysis of variance (ANOVA) was performed to analyze statistical differences. When appropriate, student's test was used to identify the significant difference between different groups. A $P$ value $< 0.05$ was considered statistically significant. All statistical analyses were performed using SPSS software (Version 22.0, SPSS Inc., Chicago, IL, USA).

**Table 3**
Pyrolysis-gas chromatography-mass spectrometry (Py-GC-MS) analysis of GTTE at 600 °C.

| No. | Rt (min) [a] | Compound | CAS No. | Content (%) [b] | SI [c] |
|---|---|---|---|---|---|
| 1 | 1.326 | Ethylamine | 75-12-7 | 31.79 | 95 |
| 2 | 1.454 | Dimethylamine | 124-40-3 | 4.82 | 92 |
| 3 | 1.541 | Ethanol | 64-17-5 | 8.82 | 93 |
| 4 | 1.727 | 1-Propen-2-ol, acetate | 108-22-5 | 0.61 | 92 |
| 5 | 1.770 | 2-methyl-Propanal | 78-84-2 | 0.36 | 82 |
| 6 | 1.815 | 2-Butene-1,4-diol | 6117-80-2 | 0.42 | 83 |
| 7 | 1.852 | 2,3-Butanedione | 431-03-8 | 1.98 | 97 |
| 8 | 1.929 | 2-methyl-Furan | 534-22-5 | 3.57 | 95 |
| 9 | 1.984 | Acetic acid | 64-19-7 | 4.16 | 97 |
| 10 | 2.080 | 2-methyl-Propanenitrile | 78-82-0 | 0.72 | 87 |
| 11 | 2.180 | 1,3-Cyclohexadiene | 592-57-4 | 0.77 | 94 |
| 12 | 2.310 | Methoxyacetonitrile | 1738-36-9 | 0.58 | 83 |
| 13 | 2.367 | 1-hydroxy-2-Propanone | 116-09-6 | 3.33 | 96 |
| 14 | 2.600 | 3-methyl-2-Butanone | 563-80-4 | 0.68 | 93 |
| 15 | 2.697 | 2,3-Pentanedione | 600-14-6 | 0.46 | 96 |
| 16 | 2.802 | 2,5-dimethyl-furan | 625-86-5 | 0.39 | 88 |
| 17 | 2.860 | 3-hydroxy-2-Butanone | 513-86-0 | 0.27 | 89 |
| 18 | 2.907 | 2,4-Dimethylfuran | 3710-43-8 | 0.34 | 92 |
| 19 | 3.046 | 2,5-dimethy-furan | 625-86-5 | 0.29 | 88 |
| 20 | 3.165 | 3-methyl-Butanenitrile | 625-28-5 | 0.27 | 96 |
| 21 | 3.261 | 1-methyl-Pyrrole | 96-54-8 | 0.20 | 85 |
| 22 | 3.489 | Pyrrole | 109-97-7 | 0.62 | 96 |
| 23 | 3.489 | Toluene | 108-88-3 | 0.81 | 97 |
| 24 | 4.155 | n-Hexyl acetate | 142-92-7 | 0.38 | 84 |
| 25 | 5.050 | 2-Cyclopenten-1-one | 930-30-3 | 0.31 | 95 |
| 26 | 5.266 | *cis*-3-Hepten-1-ol | 1708-81-2 | 0.41 | 81 |
| 27 | 5.706 | Ethylbenzene | 100-41-4 | 0.36 | 92 |
| 28 | 5.928 | Methyl benzyl ketone | 103-79-7 | 0.72 | 80 |
| 29 | 6.510 | Phenethylene | 100-42-5 | 0.23 | 86 |
| 30 | 9.242 | Phenol | 108-95-2 | 0.37 | 95 |
| 31 | 9.305 | 1-Octanol | 111-87-5 | 0.24 | 88 |
| 32 | 10.062 | 1,2,5,6-Tetrahydropyridin-2-one | 0-00-0 | 0.24 | 83 |
| 33 | 11.565 | Heptanal | 111-71-7 | 0.21 | 78 |
| 34 | 12.774 | Xanthosine | 146-80-5 | 0.38 | 80 |
| 35 | 12.904 | 1-Tetradecene | 1120-36-1 | 0.20 | 89 |
| 36 | 14.575 | 2,3-dimethyl-Cyclohexanol | 1502-24-5 | 0.22 | 65 |
| 37 | 15.099 | 1-Tetradecene | 1120-36-1 | 0.03 | 90 |
| 38 | 16.015 | 1-Hexadecene | 629-73-2 | 0.03 | 91 |
| 39 | 16.863 | 1-Pentadecene | 13360-61-7 | 0.04 | 91 |
| 40 | 17.425 | n-Octyl ether | 629-82-3 | 0.11 | 93 |
| 41 | 18.291 | n-Octyl caprylate | 2306-88-9 | 0.17 | 92 |
| 42 | 18.990 | Caffeine | 58-08-2 | 27.48 | 96 |
| 43 | 19.057 | 1-Hexadecanol | 36653-82-4 | 0.22 | 95 |
| 44 | 19.592 | Dibutyl phthalate | 84-74-2 | 0.26 | 95 |
| 45 | 19.640 | Hexadecamethylheptasiloxane | 541-01-5 | 0.24 | 65 |
| 46 | 20.416 | 1-Eicosanol | 629-96-9 | 0.20 | 94 |
| 47 | 20.937 | Octanoic acid, tetradecyl ester | 16456-36-3 | 0.04 | 63 |
| 48 | 21.254 | 1-Propyldodecyl octanoate | 0-00-0 | 0.03 | 74 |
| 49 | 21.387 | Hexadecamethylheptasiloxane | 541-01-5 | 0.04 | 78 |
| 50 | 21.877 | 2-Propenoic acid, 3-(4-methoxyphenyl)-, 2-ethylhexyl est Parsol MCX | 5466-77-3 | 0.12 | 80 |
| 51 | 22.644 | Hexadecyl 2-ethylhexanoate | 59130-69-7 | 0.06 | 89 |
| 52 | 22.810 | Carbonic acid, decyl 2-ethylhexyl ester | 0-00-0 | 0.14 | 85 |
| 53 | 23.048 | Di-*n*-octyl phthalate | 117-84-0 | 0.14 | 95 |
| 54 | 23.416 | 1-Ethylhexanoic anhydride | 36765-89-6 | 0.09 | 78 |
| 55 | 24.571 | Bis(2-ethylhexyl) isophthalate | 137-89-3 | 0.06 | 87 |

Note.
[a] Rt, retention time of pyrolytic product.
[b] The relative contents of pyrolytic products were calculated by peak area normalization, and results are expressed as the ratio of single constituent area to total area.
[c] SI, index of similarity.

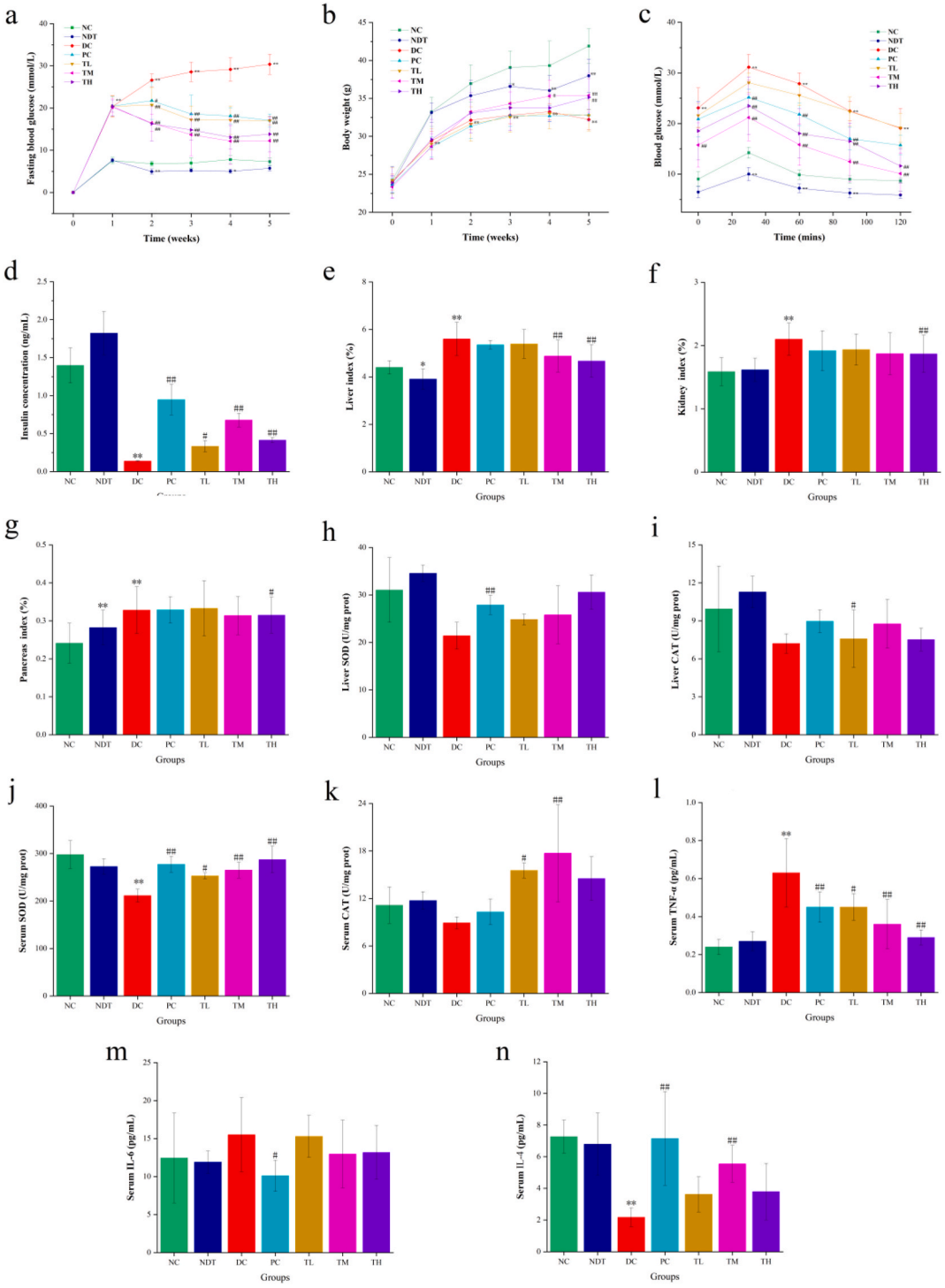


**Fig. 1.** GTTE attenuated STZ-induced diabetes-related symptoms (n = 7). (a) FBG. (b) Body weight. (c) OGTT. (d) Serum insulin. (e) Liver index. (f) Kidney index. (g) Pancreas index. (h) Liver SOD. (i) Liver CAT. (j) Serum SOD. (k) Serum CAT. (l) Serum TNF-α. (m) Serum IL-6. (n) Serum IL-4. Data are expressed as mean ± standard deviation (SD). ANOVA was performed to analyze statistical differences. $*P < 0.05$, $**P < 0.01$ vs NC group (contained NDT vs NC, DC vs NC), $\#P < 0.05$, $\#\#P < 0.01$ vs DC group (contained PC vs DC, TL vs DC, TM vs DC, TH vs DC). Note: DC = diabetic control group; PC = positive control group; NC = normal control group; TH = diabetic with high dose GTTE group; TM = diabetic with medium dose GTTE group; TL = diabetic with low dose GTTE group; NDT = nondiabetic with GTTE group; the same in Fig. 2.

## 3. Results

### 3.1. Phytochemical compositions of extract GTTE

The phytochemical components of GTTE are shown in Table 1. It contented high percentage of polysaccharide (16.93%), protein (10.15%), total polyphenols (13.90%), total amino acids (5.89%), caffeine (1.83%), and small amount of flavonoids (0.67%). For the free amino acids in GTTE, the contents of glutamate (1.04%), aspartate (0.75%), serine (0.46%), and glycine (0.44%) were relatively higher than that of other free amino acids (0.14%–0.36%). However, almost half of GTTE contained tea pigments, i.e., theabrownin (TB) (49.18%), theaflavin (0.25%), but no thearubigin.

### 3.2. Pyrolysis-gas chromatography-mass (Py-GC-MS) spectrometry analysis of GTTE

The Py-GC-MS analyses results are shown in Tables 2 and 3. As shown in Table 2, ethylamine (16.73%), acetic acid (11.82%), ethanol (10.45%), 3-oxo-butanenitrile (9.97%), 5-Amino-6-nitroso-2,4(1H,3H)-pyrimidin (7.02%), 1-hydroxy-2-propanone (4.77%), and 2,3-butanedione (2.04%) were the high content compounds produced from the decomposition at the pyrolysis temperature 380 °C and 600 °C. The ethylamine should be derived from the decompositions of free amino acids, for example, the decarboxylation of alanine generates ethylamine. Amino acids could also be generated from the pyrolysis of protein and TB. The content of caffeine was the highest at 29.47%. As caffeine is heat stable with very little decomposition resulting high percentage, caffeine should be the major component. When the sample was heated at 600 °C (Table 3), ethylamine (31.79%), ethanol (8.82%), dimethylamine (4.82%), acetic acid (4.16%), 2-methyl-furan (3.57%), 1-hydroxy-2-propanone (3.33%), and 2,3-butanedione (1.98%) were the highest content compounds from the heat decomposition. Ethylamine production was almost doubled at this high pyrolysis temperature, indicating the further decompositions of protein and amino acids in the complex. Caffeine (27.48%) was decomposed only slightly at 600 °C.

### 3.3. Effect of GTTE on feed intake, fasting blood glucose (FBG), body weight, glucose tolerance, serum insulin level, organ index, anti-oxidation ability and pro-inflammatory cytokines

The feed intake data was attached in Supplementary Material S2 Table 3 & Fig. 1. In the adaptive week and creating T1DM week, feed intake amount of all the groups were not different. In the first week after GTTE administration, DC group's feed intake showed significant ($P < 0.05$) more than that of NC group. TH group showed significant ($P < 0.05$) less than DC group. In the second week after administration, PC group showed higher ($P < 0.05$) feed intake than NC group. TM group showed less ($P < 0.05$) feed intake than DC group. In the third week after administration, PC group showed significant higher ($P < 0.01$) feed intake than NC group, and higher ($P < 0.05$) than DC group. Maybe metformin treated T1DM mice' conditions were improved, resulting more feed eating. TL group ate less ($P < 0.05$) than DC group, yet TM group ate more ($P < 0.05$) than NC group in this period. In the fourth week after administration, both PC group ($P < 0.05$) and DC group ($P < 0.01$) showed more feed intake than NC group. Yet TL and TH groups took less ($P < 0.01$) feed than DC group. Generally, DC group T1DM mice took more feed than NC group, significantly and not significantly (in the second and third weeks after administrations). Yet GTTE administration groups (TL, TM, and TH) showed less feed intake than DC group,

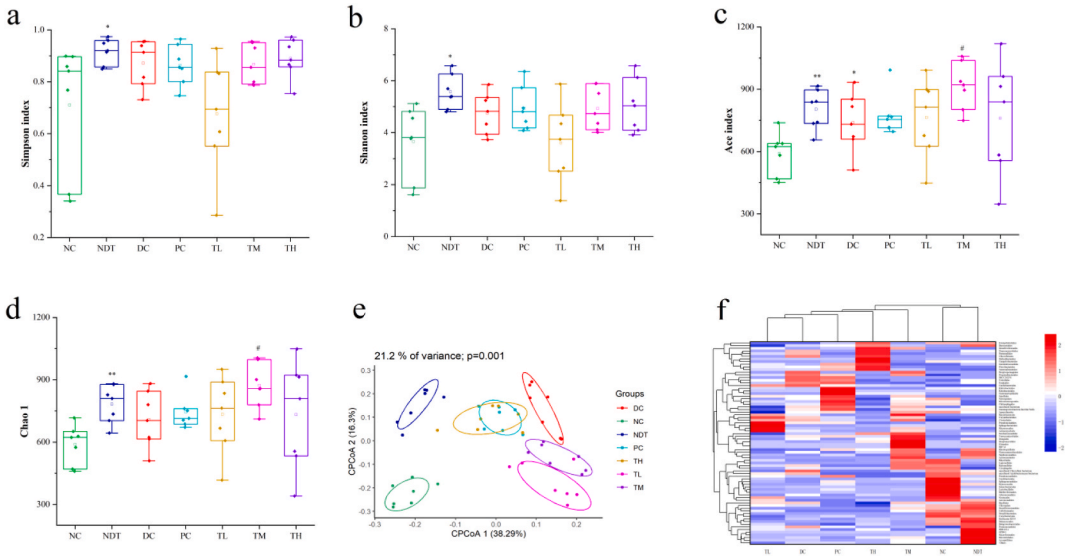


**Fig. 2.** Effects of GTTE on alpha diversity. (a) Shannon index, (b) Simpson index, (c) Ace index, (d) Chao1 index. (e) PCoA. (f) HCA. Data are expressed as mean ± standard deviation (SD). Student's test was used to identify the significant difference between different groups. $*P < 0.05$, $**P < 0.01$ vs NC group (contained NDT vs NC, DC vs NC), $\#P < 0.05$, $\#\#P < 0.01$ vs DC group (contained PC vs DC, TL vs DC, TM vs DC, TH vs DC).

significantly and not significantly. GTTE administration groups' feed intake was not different to NC group (except TM group in the third week). These feed intake results implied that GTTE could attenuate polyphagia symptom of T1DM mice.

The dynamic monitoring of fasting blood glucose (FBG) levels is presented in Fig. 1a. Compared with the NC group, FBG levels in the diabetic groups were significantly increased ($P < 0.01$) in the first week, indicating that the type 1 diabetic mice model was successfully established. At the beginning, the same FBG states were exhibited in DC group and different treatment groups. The FBG levels of the groups with different dosages of GTTE and PC group were gradually decreased from week 1 to week 5. On week 2, 3, 4 and 5, PC, TL, TM and TH groups showed significant reduction effects of the FBG levels ($P < 0.05$), compared with that of DC group. This was especially evident for the TM group, which displayed much lower FBG levels than that of other treatment groups. This result showed that GTTE could cause the decrease of the FBG levels of diabetic mice. Furthermore, the medium dose of GTTE (450 mg/kg BW, TM) had the best effect to reduce FBG levels of diabetic mice.

As shown in Fig. 1b, the same body weight trends are exhibited in 7 groups before pharmaceutical interventions. From week 0–5, the body weight of NC mice was continuously increased, while that of mice in all other groups was increased slowly compared with those in the NC group. From week 0–5, a significant decrease in the body weight of mice in DC group was observed compared with the NC group ($P < 0.01$). However, TM and TH groups showed higher body weight than those of DC group from week 2–5, especially in the TM group in week 5 ($P < 0.01$). These results indicate that GTTE can significantly alleviate the weight loss caused by type 1 diabetes.

The oral glucose tolerance test (OGTT) of GTTE on diabetic mice is shown in Fig. 1c. The blood glucose of DC group mice was significantly increased within 30 min after oral gavage of glucose, yet TM and TH group significantly reduced the blood glucose level in comparison to DC group ($P < 0.01$). After oral gavage glucose for 120 min, the blood glucose level of TM and TH group were all significantly lower than that of DC group ($P < 0.01$). These results indicated that GTTE could significantly improve glucose intolerance in diabetic mice.

As shown in Fig. 1d, the DC group showed a significant drop in the serum insulin level compared with the NC group ($P < 0.01$). On the contrary, PC, TM, TL, and TH groups remarkably increased the serum insulin levels comparative to the DC group ($P < 0.01$).

The effects of GTTE on the organ indexes (including liver, kidney and pancreas) of diabetic mice were determined. The organ indexes of liver, kidney and pancreas of DC group were all significantly increased compared with NC group (Fig. 1e,f,g, $P < 0.01$). Compared with DC group, the liver indexes of the TM group and TH group were significantly decreased ($P < 0.01$), and kidney and pancreas index in TH group were statistically different ($P < 0.05$). These results indicated that GTTE had a protective effect on the liver, kidney and pancreas of mice.

The effects of GTTE on the antioxidant enzymes in the liver and serum were measured, as shown in Fig. 1h,i,j,k. The DC group reduced the SOD and CAT activities in the liver and serum as compared with that of the NC group. Compared with the DC group, the levels of SOD and CAT in liver and serum in TL, TM, and TH treatment groups were increased with varying degrees, indicating that GTTE had positive effects on antioxidant capacity.

In order to investigate the effect of GTTE on pro-inflammatory cytokines, serum levels of tumor necrosis factor-α (TNF-α), interleukin-4 (IL-4), and interleukin-6 (IL-6) were detected using reagent test kit (Fig. 1l,m,n). Compared with the NC group, TNF-α in the DC group was significantly increased ($P < 0.01$), and IL-4 was significantly reduced ($P < 0.01$). Compared with DC group, TNF-α in the PC group and the TL, TM and TH groups was dramatically reduced ($P < 0.01$), IL-4 in PC and TM groups was increased ($P < 0.01$), and IL-6 in PC group was significantly reduced ($P < 0.05$). Although not statistically significant, the TM and TH group reduced the IL-6 level compared with the DC group. The results showed that the GTTE could significantly improve the inflammatory conditions of diabetic mice.

### 3.4. Effects of GTTE on liver and pancreatic pathology

The liver tissue status of the mice was observed under a microscope at 400 times (Supplementary Material S3 Fig. 2a). The NC group showed that the liver lobules were clearly structured clearly with neatly arranged liver cords, and liver cells were filled with cytoplasm and exhibited normal morphology and structure. In addition, liver sinusoids were not significantly expanded or compressed. In the DC group, the fibrosis of liver tissue was increased, with the central vein of the liver lobule and the nearby hepatic sinusoids highly dilated and congested, and the liver cells displayed balloon-like degeneration. Compared with DC group, the PC and GTTE administration groups apparently alleviated the fibrosis of liver tissue and improved the morphology of the liver cells.

The morphology of mice pancreas was observed under a microscope at 400 times (Supplementary Material S3 Fig. 2b). Both the NC and NDT group showed that the pancreatic acinar and pancreatic islets were normal. The pancreatic islet tissue was intact with complete morphology. The pancreatic islet cells were cord-shaped, round or oval, with abundant cytoplasm, clear borders, centered nucleus and clear borders between cells. The number of pancreatic islet cells in DC group decreased, with irregularly shaped cells and disordered and scattered cell arrangement. The edges of the cells were uneven, with blurred boundaries, enlarged cell volume, and pancreatic acinar. The PC and GTTE administration groups exhibited better repair alterations of islet cells and pancreas. Compared with DC group, the number of islet cells in the GTTE administration group increased, and the state of pancreatic tissue was significantly improved.

### 3.5. Effects of GTTE on islet β-cells areas

The effects of GTTE on the insulin and glucagon in the pancreas are shown in immunoreaction images in Supplementary Material S3 Fig. 3a,b,c. Compared with normal NC group, the area of islet α-cells in the DC group was significantly increased, and the area of islet β-cells was significantly reduced ($P < 0.01$). Compared with the DC group, the PC and TL group decreased the area of islet α-cells

and increased the area of islet β-cells, but the difference was not statistically significant ($P > 0.05$). The TM and TH groups had significantly decreased islet α-cells area and increased islet β-cells area ($P < 0.01$).

### 3.6. Effects of GTTE on gut microbiota

#### 3.6.1. Community diversity analysis

The gut microbiota community diversity of the seven groups' feces samples was assessed based on alpha diversity and beta diversity. Alpha diversity reflects the richness and diversity of microbial community, including Ace index, Chao1 index, Shannon index and Simpson index (Fig. 2a,b,c,d). Among them, the Ace index and Chao1 index, as the abundance index, reflect the number of bacteria in the feces samples. The Shannon index and Simpson index reflect the index of bacterial diversity in the feces samples. The DC group elevated the Ace, Chao1, Shannon, and Simpson indexes compared with NC group, and the difference was statistically significant ($P \geq 0.05$), except in Ace index. Compared with DC group, the Ace and Chao1 indexes were increased in TL, TM, TH groups. Although these differences were not statistically significant ($P \geq 0.05$), but TM group was significant ($P < 0.05$). The indexes of Shannon and Simpson of TH group showed an upward trend, but TL group showed a downward trend ($P \geq 0.05$). These trends indicated that the effects of GTTE on bacterial diversity could be relevant to its proper dosage. The upward trends indicated that GTTE administrations can increase the diversity and abundance of the gut microbiota of diabetic mice.

Beta diversity can reflect differences in the microbial communities of samples. UniFrac distance-based principal coordinate analysis (PCoA) was used to reveal the distinct clustering of intestinal microbe communities for each experimental group. The DC group was deviated from the NC group according to the microbiota composition, indicating that the composition of the gut microbiota of diabetic model mice had changed (Fig. 2e). Additionally, both the PC and GTTE administration groups had the trend closing to the NC group, and they all departed from DC group, which indicated that GTTE administration could reduce the damage of gut microbiotia of diabetic mice induced by STZ. Furthermore, TH group was more close to the NC group than that of TL and TM groups. This indicated that high doses of GTTE administration had a more significant effect on improving gut microbiota imbalance. The results of PCoA largely agreed with that of the hierarchical clustering analysis (Fig. 2f).

#### 3.6.2. Gut microbiota composition

To further investigate the specific changes in bacterial communities, the relative abundance of the predominant phyla and genera was compared across seven groups, especially taxa responding to GTTE administration (Supplementary Material S3 Fig. 4). At the phylum level, the structures of seven groups of microbial communities were mainly composed of bacteroidetes and Firmicutes, fllowed by Actinobacteria and Proteobacteria (Supplementary Material S3 Fig. 4a). The contents of Bacteroidetes and Firmicutes in the total flora were 90%, 66%, and 42%–87% in the NC, DC, and GTTE groups, respectively. Compared with NC group, the ratio of Firmicutes to Bacteroidetes (F/B) and the abundance of Firmicutes were significantly reduced ($P < 0.01$, Supplementary Material S3 Fig. 4b–d). The abundance of Bacteroidetes and Actinobacteria were increased in DC group (Supplementary Material S3 Fig. 4c and d). In TL and TM groups, the F/B ratio and the abundance of Actinobacteria showed an upward trend compared with DC group (Supplementary Material S3 Fig. 4d and e). Additionally, the abundance of Bacteroidetes was increased, while Actinobacteria was decreased, along with the increasing of GTTE administration dose in treatment groups. These opposite trend maybe reflect the dosage effect of GTTE. The abundance of Proteobacteria showed no significant difference among NC, DC, TL, TM and TH (Supplementary Material S3 Fig. 4f). At the genus level, the dominant bacteria genera in NC and NDT groups were Lactobacillus, Alistipes, Ruminococcaceae UCG-014, and Psychrobacter (Supplementary Material S3 Fig. 4g). In the DC group, the dominant bacteria were Corynebacterium, Lactobacillus, Psychrobacter, and Lachnospiraceae NK4A136 group. The abundance of Corynebacterium, Lactobacillus, Lachnospiraceae NK4A136 group in GTTE administration groups were more than other bacteria. However, a little content of Corynebacterium was observed in NC and NDT groups. Compared with NC group, the abundance of Corynebacterium and Psychrobcuter were increased and the content of Lactobacillus and Alistipes reduced in DC group (Supplementary Material S3 Fig. 4h,i,j,l). The abundance of Lactobacillus and Lachnospiraceae NK4A136 group of GTTE administration groups were increased in comparison with DC group but did not reach statistical significance (Supplementary Material S3 Fig. 4i–k). Psychrobacter was increased in TL group and reduced in TL and TH group. These results showed that the changes in various gut microbiota were caused in the DC group, but the administration of GTTE can improve this trend.

## 4. Discussion

"Golden-flower" Tibetan tea (GTT) is an innovative dark tea fermented via fungus Eurotium cristatum. It belongs to the category of post-fermentation tea, which generates abundant phytochemicals in the fermentation stage. TB is a major component in GTTE. In recent years, studies have exhibited that TB possesses inhibitory activity on α-glucosidase in vitro, reductes blood glucose levels and improves glucose tolerance in mice under hyperglycemic stress [23], indicating its health benefits to diabetes mellitus (DM). Theaflavins show inhibitory effects on α-glucosidase and α-amylase activity resulting in decreased plasma levels of glucose [24]. Thus, tea pigments may play an important role for the antidiabetic effects of GTTE. Polysaccharides should not only directly play a role for the health benefits of the dark tea but also be used by gut microbiota to turn into short-chain fatty acids (SCFAs) via saccharolytic fermentation [25]. Polyphenols also contribute to health benefits. Although total polyphenols content was high, there were only a total of 1.32% of specific tea phenolic compounds in GTTE, including GC (0.51%), GA (0.48%), and EC (0.11%). This was in line with the literature's reports [26] that tea phenolic compounds were transformed to tea pigments or other complex in the fermentation processes of dark tea.

In addition, caffeine can increase glucose transporter IV expression [27]. A meta-analysis of prospective studies reported that caffeine intake might significantly reduce the incidence of T2DM [28]. Thus, caffeine was also a contributor to the antidiabetic effects.

The Py-GC-MS analyses results further exhibit the insight that the large complex substance, such as theabrownin, in GTTE contains phenols, acids, organic hydrocarbons, aromatic compounds, ketones, alcohols, aldehydes, and nitrogen compounds, mainly composed of phenols, lipids, sugars, and proteins.

Overall, it is reasonable to conclude that all these phytochemical components could synergistically contribute to the antidiabetic effects of GTTE.

Type 1 diabetes is caused by an absolute deficiency of insulin secretion. FBG level, OGTT, and insulin resistance are important indicators of diabetes alleviation [29,30]. In this study, at some point in the beginning, DC group exhibited more feed intake, higher level of FBG and blood glucose, and lower serum insulin compared with those of the NC group. These results were in agreement with another report [31] that STZ rat models with raised blood glucose levels coexists with either the same, lower or higher levels of insulin as compared with control. After a period of GTTE administrations, the GTTE groups reduced the elevated FBG and blood glucose level, and increased the depressive serum insulin levels. It is reported that drugs with hypoglycemic effect usually had obvious effects on reducing the FBG, improving glucose intolerance and increasing the serum insulin levels [32,33]. The reversal effects were especially evident on FBG level for TM group, on glucose tolerance for TM and TH group, on serum insulin for TM and TH group, respectively. These results indicate that GTTE could improve the symptoms of diabetes.

The STZ induced diabetic mice group (DC) showed drastic weight loss after STZ induction when compared with that of normal diet group (NC) group. This may be due to defects in glucose metabolism and excessive breakdown of tissue protein and fat [31]. However, the diabetic mice treated with GTTE (TM and TH groups) significantly prevented the body weight loss. The liver, kidney, and pancreas indexes of the TH group were significantly decreased. The organ weights could reflect the body's pathological conditions and inflammation [34]. These results indicated that the GTTE could ameliorate the decrease of body weight and alleviate the pathological changes of organs of diabetic mice.

Various studies have shown that oxidative stress plays an important role in the pathology of diabetes [35]. It is not just because of its role in the development of complications, but also because persistent hyperglycemia, secondary to insulin resistance, may induce oxidative stress and contribute to β-cell destruction in diabetes [36,37]. In this study, the antioxidant potency of GTTE was investigated via estimating the antioxidant enzymes SOD and CAT. These two enzymes can reduce oxidative stress, inhibit the proliferation of peroxisome and improve islets β-cell damage [38,39]. Compared with the DC group, the levels of SOD and CAT in the liver and blood of GTTE groups increased in varying degrees, indicating that the extract from the "Golden-flower" Tibetan tea could stimulate the defense mechanism of oxidative stress and reduce oxidative stress in vivo.

Inflammatory cytokines play an important role in the pathogenesis of insulin resistance. As the intermediate hub of the immune response, pro-inflammatory cytokines directly produce toxic effects on pancreatic β-cells and affect the body by activating the inflammatory cytokines signaling pathway [40,41]. As such, decreasing of inflammatory factors and the increasing of anti-inflammatory factors can effectively alleviate the occurrence and development of diabetes. Furthermore, disturbance of the homeostasis between the pro- and anti-inflammatory cytokines leads to T1DM [42]. In this study, the results showed that the proinflammatory cytokines levels of TNF-α were down-regulated, and the anti-inflammatory level of IL-4 was up-regulated, which indicated that the GTTE might have the potential to alleviate the development of diabetes. There was also report [43] that inhibiting the release of inflammatory factors could repair insulin signaling pathways and reduce blood sugar.

According to the histopathological analysis, diabetes causes the destruction of the pancreas [41]. In addition to the pancreas, the liver plays an important role in maintaining blood glucose balance by storing glucose as glycogen and producing glucose through glycogen degradation and gluconeogenesis [44]. In the present study, GTTE showed a favorable protective effect on the liver and repair of islet cells and pancreas. Compared with DC group, the PC and GTTE groups alleviated the fibrosis of liver tissue, improved the morphology of the liver cell, increased the number of islet cells, and improved the state of pancreatic tissue.

In order to further understand the mechanism of GTTE on the blood glucose regulation in diabetic mice, this study observed the relative positive area of islet α-cells and islet β-cells. Previous studies have shown that islet α-cells secrete glucagon, which affect glycogen breakdown and gluconeogenesis, and interact with insulin secreted by islet cells to maintain the body's blood sugar balance [45]. The body's high blood sugar will destroy the islet β-cells, increase glucagon secretion and decrease insulin secretion [29]. After 4 weeks of administrations, TM and TH groups significantly increased the area of pancreatic islet β-cells and decreased the area of pancreatic islet α-cells ($P < 0.05$), which should be led by the continued low blood sugar levels to protect their islet β-cells.

The gut microbiota plays a vital role in the physiology and pathology of the host, especially associated with the pathogenesis of metabolic diseases such as obesity, insulin resistance and diabetes [46]. Nowadays, more and more evidence has shown that dietary factors profoundly modulate gut microbiota, which further mediates the biological function of the dietary factors [47]. Therefore, the 16S rDNA amplicon sequencing was performed to analyze the changes in gut microbiota of different GTTE intervention groups. The upward trends of alpha diversity in GTTE groups reflect that GTTE administration could increase the diversity and abundance of gut microbiota of mice. Similarly, beta diversity analysis demonstrated a clear separation of the DC group from the NC group. The GTTE group also deviated from the DC group, indicating that GTTE could regulate the intestinal microbial community to develop toward the NC group.

Results showed that gut microbiota composition was improved. Bacteroidetes and Firmicutes are the dominant flora, followed by Actinobacteria and Proteobacteria. Firmicutes and Bacteroidetes can convert indigestible carbohydrates into short-chain fatty acids (SCFAs) in the intestines, mainly propionic acid and butyric acid [48]. SCFAs are a class of beneficial metabolites produced by gut microbiota. The deficiency of SCFAs could be associated with metabolic diseases, including obesity and diabetes [49]. The Firmicutes to Bacteroidetes (F/B) ratio is associated with the development of metabolic disorder. Bacteroidetes was reported in children who

developed T1DM [50]. Patients with T1DM were also found the high abundance of Bacteroides [51,52]. In present study, the relevant abundance of Bacteroides was 28%, 37% and 14%, in NC, DC, and TL groups, respectively. This indicates that low dose GTTE administration induced a lower abundance of Bacteroides. Additionally, the F/B ratio decreased in DC group, and increased in TL, and TM groups. Giongo et al. [53] reported that the F/B ratio was decreased with the lapse of time in the T1DM cases. Previous research has found that the higher F/B ratio was conducive to the decomposition of polysaccharides [54]. Furthermore, the relevant abundance of Bacteroidetes increased and Actinobacteria (related with a series of inflammatory reactions [55]) reduced as with the increasing of GTTE dosage. This dose effect indicated that different dosages of GTTE might have different alleviating effects on diabetes. Proteobacteria includes a series of pathogenic bacteria such as Salmonella and Vibrio cholerae, which may cause disturbance of the intestinal microflora and affect the health of the host [56]. Here, the relevant abundance of Proteobacteria was 7.6%, 7.2%, 5.7%, 2.8% and 2.9% in NC, DC, TL, TM and TH groups, respectively. The results indicate that GTTE administration can inhibit the proliferation of Proteobacteria. In the study, the GTTE with different dosages exhibited different effect on the same bacteria. When compared with DC group, the relevant abundance of Corynebacterium 1 and Psychrobacter was increased in TL group, and decreased in TH group. These results further suggested that the dosage of GTTE was an impact factor of the effects on the alleviation of diabetes.

The study shows comprehensive insight of GTTE phytochemical compositions. GTTE showed significant effects to alleviate the general conditions of T1DM mice. As discussed above, many of the compositions may synergistically contribute to the antidiabetic effects. Systematic mechanism was not studied in this paper. Network pharmacology approach will be useful to understand the complex pharmacological mechanisms of GTTE. The alleviating effects of GTTE to T1DM mice model can only be considered preliminary results. Other T1DM animal model, such as BB rat, could be used for further studies.

## 5. Conclusions

Extracted from “golden-flower” Tibetan tea, GTTE contains pigment theabrownin (TB) and a high percentage of tea polysaccharide, protein, polyphenols, amino acids, caffeine, and a small amount of flavonoids. GTTE can effectively alleviate the conditions of T1DM mice induced by STZ, i.e., reducing their FBG, elevating body weight, improving glucose intolerance, increasing serum insulin levels, relieving liver and pancreatic injury, restoring damaged islet cells. GTTE also improves the gut microbiota of diabetic mice by increasing the diversity and abundance of the gut microbiota, modulating gut microbiota composition by resisting changes of flora structure, increasing the abundant of beneficial bacteria such as Firmicutes, increasing the proper Firmicutes/Bacteroidetes (F/B) ratio, and reducing harmful bacteria content such as Proteobacteria. The findings suggest multi-channel mechanisms could be involved in the synergistic effects on T1DM. The pathways include decreasing oxidative stress by increasing SOD and CAD levels, modulating cytokine expression leading to the decreasing pro-inflammatory cytokines TNF-α and IL-6, increasing anti-inflammatory cytokines IL-4 to improve inflammatory responses, and improving of gut microbiota. Further study of the mechanisms is needed in the future works. These findings not only provide meaningful understandings for the health benefits of long term daily drinking “golden-flower” Tibetan tea but also provide scientific basis for the research and development of functional foods and dietary supplements originating from the “golden-flower” Tibetan tea.

## Ethics statement

The study was approved by the Institutional Animal Care and Use Committee of Sichuan University (KS20201023).

## Consent for publication

All authors consent for publication.

## Funding statement

This study was supported by the grant from Key Research and Development Program of Science and Technology Foundation of Sichuan Province, China (No. 2019YFN0178, No.2023YFN0012); 1 + 9 Unveiling of for tackling key scientific and technological problems - functional food core technology, Sichuan Academy of Agricultural Sciences (1+9KJGG007), China.

## Data availability statement

Data available within the article and its supplementary materials.

## CRediT authorship contribution statement

**Junlin Deng:** Writing – original draft, Visualization, Formal analysis. **Kebin Luo:** Writing – original draft, Software, Methodology, Data curation. **Chen Xia:** Supervision, Methodology, Investigation, Funding acquisition. **Yongqing Zhu:** Resources, Investigation, Funding acquisition. **Zhuoya Xiang:** Software, Formal analysis. **Boyu Zhu:** Software, Formal analysis. **Xiaobo Tang:** Software, Formal analysis. **Ting Zhang:** Software, Formal analysis. **Liugang Shi:** Resources. **Xiaohua Lyu:** Supervision, Conceptualization. **Jian Chen:** Writing – review & editing, Supervision, Funding acquisition, Conceptualization.

## Declaration of competing interest

The authors declare the following financial interests/personal relationships which may be considered as potential competing interests: Jian Chen reports financial support was provided by Sichuan Science and Technology Agency, China. Chen xia reports financial support was provided by Sichuan Science and Technology Agency, China. Yongqing Zhu reports financial support was provided by Sichuan Academy of Agricultural Sciences, China. If there are other authors, they declare that they have no known competing financial interests or personal relationships that could have appeared to influence the work reported in this paper.

## Appendix A. Supplementary data

Supplementary data to this article can be found online at https://doi.org/10.1016/j.heliyon.2024.e27145.

## References


[1] A.D. Association, Diagnosis and classification of diabetes mellitus, Diabetes Care 33 (Supplement_1) (2010) S62–S69, https://doi.org/10.2337/diacare.28.suppl_1.S37.
[2] W.H. Hoffman, S.A. Whelan, N. Lee, Tryptophan, kynurenine pathway, and diabetic ketoacidosis in type 1 diabetes, PLoS One 16 (7) (2021) e0254116, https://doi.org/10.1371/journal.pone.0254116.
[3] Teresa Quattrin, Lucy D. Mastrandrea, S. Lucy, K. Walker, Type 1 diabetes, Lancet 401 (10394) (2023) 2149–2162, https://doi.org/10.1016/S0140-6736(23)00223-4.
[4] Lourdes V. Cross, R. Thomas James, Safety and efficacy of dietary supplements for diabetes, Diabetes Spectr. 34 (1) (2021) 67–72, https://doi.org/10.2337/ds19-0068.
[5] D.K. Patel, S.K. Prasad, R. Kumar, S. Hemalatha, An overview on antidiabetic medicinal plants having insulin mimetic property, Asian Pac. J. Trop. Biomed. (4) (2012) 11, https://doi.org/10.1016/S2221-1691(12)60032-X.
[6] V.V. Chopade, A.A. Phatak, A.B. Upaganlawar, A.A. Tankar, Green tea (Camellia sinensis): chemistry, traditional, medicinal uses and its pharmacological activities - a review, Phcog. Rev. 2 (3) (2008) 157–162.
[7] T. Hasumura, Y. Shimada, J. Kuroyanagi, Y. Nishimura, S. Meguro, Y. Takema, T. Tanaka, Green tea extract suppresses adiposity and affects the expression of lipid metabolism genes in diet-induced obese zebrafish, Nutr. Metab. 9 (1) (2012) 73, https://doi.org/10.1186/1743-7075-9-73.
[8] H.C. Huang, J.K. Lin, Pu-erh tea, green tea, and black tea suppresses hyperlipidemia, hyperleptinemia and fatty acid synthase through activating AMPK in rats fed a high-fructose diet, Food Funct. 3 (2012) 170–177, https://doi.org/10.1039/c1fo10157a.
[9] I. Ikeda, T. Yamahira, M. Kato, A. Ishikawa, Black-tea polyphenols decrease micellar solubility of cholesterol in vitro and intestinal absorption of cholesterol in rats, J. Agric. Food Chem. 58 (15) (2010) 8591–8595, https://doi.org/10.1210/en.2006-1315.
[10] P. Xu, J. Wu, Y. Zhang, H. Chen, Y. Wang, Physicochemical characterization of puerh tea polysaccharides and their antioxidant and α-glycosidase inhibition, J. Funct.Foods 6 (2014) 545–554, https://doi.org/10.1016/j.jff.2013.11.021.
[11] G. Chen, Q. Yuan, M. Saeeduddin, S. Ou, Y. Hong, Recent advances in tea polysaccharides: extraction, purification, physicochemical characterization and bioactivities, Carbohydr. Polym. 153 (2016) 663–678, https://doi.org/10.1016/j.carbpol.2016.08.022.
[12] H. Cao, Polysaccharides from Chinese tea: recent advance on bioactivity and function, Int. J. Biol. Macromol. 62 (2013) 76–79, https://doi.org/10.1016/j.ijbiomac.2013.08.033.
[13] N. Kuhnert, Unraveling the structure of the black tea thearubigins, Arch. Biochem. Biophys. 501 (1) (2010) 37–51, https://doi.org/10.1016/j.abb.2010.04.013.
[14] Qiuping Wang, Belscak-Cvitanovic, Durgo Ana, Chisti Ksenija, Yusuf, Gong, Jiashun, Physicochemical properties and biological activities of a high-theabrownins instant Pu-erh tea produced using Aspergillus tubingensis, LWT–Food Sci. Technol. 90 (2018) 598–605, https://doi.org/10.1016/j.lwt.2018.01.021.
[15] W. Jin, L. Zhou, B. Yan, L. Yan, F. Liu, P. Tong, W. Yu, X. Dong, L. Xie, J. Zhang, Theabrownin triggers DNA damage to suppress human osteosarcoma U2 OS cells by activating p53 signalling pathway, J. Cell Mol. Med. 22 (9) (2018) 4423–4436, https://doi.org/10.1111/jcmm.13742.
[16] Heng Zhang, Feifei Zhang, Bin Zhang, Research progress on active components and functions of Ya'an Tibetan tea, Modern Food (12) (2020) 12–14 (in Chinese).
[17] A.A. Albalasmeh, A.A. Berhe, T.A. Ghezzehei, A new method for rapid determination of carbohydrate and total carbon concentrations using UV spectrophotometry, Carbohydr. Polym. 97 (2) (2013) 253–261, https://doi.org/10.1016/j.carbpol.2013.04.072.
[18] Y.S. Velioglu, G. Mazza, L. Gao, B.D. Oomah, Antioxidant activity and total phenolics in selected fruits, vegetables, and grain products, J. Agric. Food Chem. 46 (10) (1998) 4113–4117, https://doi.org/10.1021/jf9801973.
[19] A.A.L. Ordonez, J.D. Gomez, M.A. Vattuone, M.I. Lsla, Antioxidant activities of Sechium edule (Jacq.) Swartz extracts, Food Chem. 97 (3) (2006) 452–458, https://doi.org/10.1016/j.foodchem.2005.05.024.
[20] M.S. Hashemi, Z.M. Hassan, N. Hossein-Khannzer, A.K. Pourfathollah, S. Soudi, Investigating the route of administration and efficacy of adipose tissue-derived mesenchymal stem cells and conditioned medium in type 1 diabetic mice, Inflammopharmacology 28 (2) (2020) 585–601, https://doi.org/10.1007/s10787-019-00661-x.
[21] B.L. Furman, Streptozotocin-induced diabetic models in mice and rats, Current Protocols 1 (2021) e78, https://doi.org/10.1002/cpz1.78.
[22] M.W. Jing, Y.J. Ge, K.L. Liu, Study on the supplementary regulation of blood lipid by tea pigment capsules in rats, 2007, Chinese Modern Doctor 45 (5) (2007) 18–19 (in Chinese).
[23] D. Chen, J. Sun, W. Dong, Y. Shen, Z. Xu, Effects of polysaccharides and polyphenolics fractions of Zijuan tea (Camellia sinensis var. kitamura) on α-glucosidase activity and blood glucose level and glucose tolerance of hyperglycaemic mice, Int. J. Food Sci. Technol. 53 (10) (2013) 2335–2341, https://doi.org/10.1111/ijfs.13825.
[24] T. Matsui, T. Tanaka, S. Tamura, A. Toshima, K. Tamaya, Y. Miyata, K. Tanaka, K. Matsumoto, Alpha-glucosidase inhibitory profile of catechins and theaflavins, J. Agric. Food Chem. 55 (2007) 99–105, https://doi.org/10.1021/jf0627672.
[25] G.R. Gibson, Fibre and effects on probiotics (the prebiotic concept), Clin. Nutr. Suppl. 1 (2) (2004) 25–31, https://doi.org/10.1016/j.clnu.2004.09.005.
[26] Y.Y. Tu, H.L. Liang, X. Chen, Y.Y. Hu, W.F. Chen, Analysis of catechins and organic acids in compressed teas, Journal of Tea 28 (1) (2002) 22–24 (In Chinese).
[27] E. Mukwevho, T.A. Kohn, D. Lang, E. Nyatia, J. Smith, E.O. Ojuka, Caffeine induces hyperacetylation of histones at the MEF2 site on the Glut4promoter and increases MEF2A binding to the site via a CaMK-dependent mechanism, Am. J. Physiol. Endocrinol. Metab. 294 (2008) E582–E588, https://doi.org/10.1152/ajpendo.00312.2007.
[28] X.B. Jiang, D.F. Zhang, W.J. Jiang, Coffee and caffeine intake and incidence of type 2 diabetes mellitus: a meta-analysis of prospective studies, Eur. J. Nutr. 53 (2014) 25–38, https://doi.org/10.1007/s00394-013-0603-x.
[29] Z.Q. Chen, C. Wang, Y.X. Pan, X.D. Gao, H.X. Chen, Hypoglycemic and hypolipidemic effects of anthocyanins extract from black soybean seed coat in high fat diet and streptozotocin-induced diabetic mice, Food Funct. 9 (2018) 426–439, https://doi.org/10.1039/C7FO00983F.

[30] A. Hassan, N. Tajuddin, A. Shaikh, Retrospective Case series of patients with diabetes or prediabetes who were switched from omega-3-acid ethyl esters to icosapent ethyl, Cardiology & Therapy 4 (1) (2014) 1–11, https://doi.org/10.1007/s40119-014-0032-9.
[31] M.H. Al-Zuaidy, M.W. Mumtaz, A.A. Hamid, A. Ismail, S. Mohamed, A. Razis, Biochemical characterization and 1H NMR based metabolomics revealed Melicope lunu-ankenda leaf extract a potent anti-diabetic agent in rats, BMC Compl. Alternative Med. 17 (1) (2017) 359, https://doi.org/10.1186/s12906-017-1849-2.
[32] H. Li, S. Chu, H. Zhao, D. Liu, X. Liu, Q. Xi, J. Chen, Z. Li, J. Li, Effect of zishen jiangtang pill, a Chinese herbal product, on rats with diabetic osteoporosis, Evidence-Based Complementray and Alternative Medicine (2018) 1–10, https://doi.org/10.1155/2018/7201914.
[33] Z. Qin, W. Wang, D. Liao, X. Wu, X.E. Li, UPLC-Q/TOF-MS-Based serum metabolomics reveals hypoglycemic effects of rehmannia glutinosa, coptis chinensis and their combination on high-fat-diet-induced diabetes in KK-Ay mice, Int. J. Mol. Sci. 19 (12) (2018) 3984, https://doi.org/10.3390/ijms19123984.
[34] J.A. Rodriguez, K. Singh, The Spanish availability and readability of diabetes apps, J. Diabetes Sci. Technol. 12 (3) (2018) 719–724, https://doi.org/10.1177/1932296817749610.
[35] F. Giacco, M. Brownlee, Oxidative stress and diabetic complications, Circ. Res. 107 (9) (2010) 1058–1070, https://doi.org/10.1161/CIRCRESAHA.110.223545.
[36] X.L. Shen, H. Liu, H. Xiang, X.M. Qin, G.H. Du, J.S. Tian, Combining biochemical with 1 H NMR-based metabolomics approach unravels the antidiabetic activity of genipin and its possible mechanism, J. Pharmaceut. Biomed. Anal. 129 (2016) 80–89, https://doi.org/10.1016/j.jpba.2016.06.041.
[37] A. Saha, S. Mazumder, An aqueous extract of Murraya koenigii leaves induces paraoxonase 1 activity in streptozotocin induced diabetic mice, Food Funct. 4 (2013) 420–425, https://doi.org/10.1039/c2fo30193h.
[38] C. Cao, B. Zhang, C. Li, Q. Huang, X. Fu, Structure and in vitro hypoglycemic activity of a homogenous polysaccharide purified from Sargassum pallidum, Food Funct. 10 (2019) 2828–2838, https://doi.org/10.1039/c8fo02525h.
[39] J.F. Gu, Z.Y. Zheng, J.R. Yuan, B.J. Zhao, C.F. Wang, L. Zhang, Q.Y. Xu, G.W. Yin, L. Feng, X.B. Jia, Comparison on hypoglycemic and antioxidant activities of the fresh and dried Portulaca oleracea L. in insulin-resistant HepG2 cells and streptozotocin-induced C57BL/6J diabetic mice, J. Ethnopharmacol. 161 (2015) 214–223, https://doi.org/10.1016/j.jep.2014.12.002, 2015.
[40] A. Amrani, J. Verdaguer, S. Thiessen, S. Bou, P. Santamaria, IL-1alpha, IL-1beta, and IFN-gamma mark beta cells for Fas-dependent destruction by diabetogenic CD4(+) T lymphocytes, J. Clin. Invest. 105 (4) (2000) 459, https://doi.org/10.1172/JCI8185.
[41] A. Rabinovitch, W.L. Suarez-Pinzon, Cytokines and their roles in pancreatic islet β-cell destruction and insulin-dependent, Diabetes Mellitus 55 (8) (1998) 1139–1149, https://doi.org/10.1016/s0006-2952(97)00492-9.
[42] Alex, Rabinovitch, An update on cytokines in the pathogenesis of insulin-dependent diabetes mellitus, Diabetes Metab. Rev. 14 (2) (1998) 129–151, https://doi.org/10.1002/(SICI)1099-0895(199806)14:2<129::AID-DMR208>3.0.CO;2-V.
[43] Y.B. Li, W.H. Zhang, H.D. Liu, S.P. Ma, Protective effects of Huanglian Wendan Decoction aganist cognitive deficits and neuronal damages in rats with diabetic encephalopathy by inhibiting the release of inflammatory cytokines and repairing insulin signaling pathway in hippocampus, Chin. J. Nat. Med. 14 (11) (2016) 10. CNKI:SUN:ZGTR.0.2016-11-003.
[44] M. Roden, E. Bernroider, Hepatic glucose metabolism in human-its role in health and disease, Best Pract. Res. Clin. Endocrinol. Metabol. 17 (3) (2003) 365–383, https://doi.org/10.1016/s1521-690x(03)00031-9.
[45] S.J.L. Marchand, D.W. Piston, Glucose Suppression of Glucagon Secretion metabolic and calcium responses from α-cells in intact mouse pancreatic islets, J. Biol. Chem. 285 (19) (2010) 14389, https://doi.org/10.1074/jbc.M109.069195.
[46] V. Lazar, L.M. Ditu, G.G. Pircalabioru, A. Picu, M.C. Chifiriuc, Gut microbiota, host organism, and diet trialogue in diabetes and obesity, Front. Nutr. 6 (2019) 21, https://doi.org/10.3389/fnut.2019.00021.
[47] J. Benjamino, S. Lincoln, R. Srivastava, J. Graf, Low-abundant bacteria drive compositional changes in the gut microbiota after dietary alteration, Microbiome 6 (1) (2018) 1–13, https://doi.org/10.1186/s40168-018-0469-5.
[48] T.A. Houtman, H.A. Eckermann, H. Smidt, C. deWeerth, Gut microbiota and BMI throughout childhood: the role of firmicutes, bacteroidetes, and short-chain fatty acid producers, Sci. Rep. 12 (1) (2022) 1–13, https://doi.org/10.1038/s41598-022-07176-6.
[49] J.J. Qin, Y.R. Li, Z.M. Cai, S.H. Li, J.F. Zhu, F. Zhang, et al., A metagenome-wide association study of gut microbiota in type 2 diabetes, Nature 490 (7418) (2012) 55–60, https://doi.org/10.1038/nature11450.
[50] C.T. Brown, A.G. Davis-Richardson, A. Giongo, K.A. Gano, D.B. Crabb, N. Mukherjee, G. Casella, J.C. Drew, J. Ilonen, M. Knip, Gut microbiome metagenomics analysis suggests a functional model for the development of autoimmunity for type 1 diabetes, PLoS One 6 (10) (2011) e25792, https://doi.org/10.1371/journal.pone.0025792.
[51] M.E. Mejía-León, J.F. Petrosino, N.J. Ajami, M.G. Domínguez-Bello, A.M. de la Barca, Fecal microbiota imbalance in Mexican children with type 1 diabetes, Sci. Rep. 4 (2014) 3814, https://doi.org/10.1038/srep03814.
[52] M.C. de Goffau, S. Fuentes, B. van den Bogert, H. Honkanen, W.M. de Vos, G.W. Welling, H. Hyöty, H.J. Harmsen, Aberrant gut microbiota composition at the onset of type 1 diabetes in young children, Diabetologia 57 (8) (2014) 1569–1577, https://doi.org/10.1007/s00125-014-3274-0.
[53] A. Giongo, K.A. Gano, D.B. Crabb, N. Mukherjee, L.L. Novelo, G. Casella, J.C. Drew, J. Ilonen, M. Knip, H. Hyöty, R. Veijola, T. Simell, O. Simell, J. Neu, C. H. Wasserfall, D. Schatz, M.A. Atkinson, E.W. Triplett, Toward defining the autoimmune microbiome for type 1 diabetes, ISME J. 5 (2011) 82–91, https://doi.org/10.1038/ismej.2010.92.
[54] L. Ming, Y.F. Wang, G.W. Fan, X.Y. Wang, S.Y. Xu, Y. Zhu, Balancing herbal medicine and functional food for prevention and treatment of cardiometabolic diseases through modulating gut microbiota, Front. Microbiol. 8 (2017) 2146, https://doi.org/10.3389/fmicb.2017.02146.
[55] Q. Ma, Y. Li, J. Wang, P. Li, Y. Duan, H. Dai, Y. An, L. Cheng, T. Wang, C. Wang, T. Wang, B. Zhao, Investigation of gut microbiome changes in type 1 diabetic mellitus rats based on high-throughput sequencing, Biomed. Pharmacother. 124 (2020) 109873. http://doi:10.1016/j.biopha.2020.109873.
[56] N.R. Shin, T.W. Whon, J.W. Bae, Proteobacteria: microbial signature of dysbiosis in gut microbiota, Trends Biotechnol. 33 (9) (2015) 496–503, https://doi.org/10.1016/j.tibtech.2015.06.011.